Materials Characterization xxx (xxxx) 112158

Contents lists available at ScienceDirect

Materials Characterization

journal homepage: www.elsevier.com/locate/matchar

Application of electron backscatter diffraction in facet crystalline orientation study of Al-Cu-Fe alloy

Chunfei Li*, Josiah Dubovi, Clay Klein

Clarion University of Pennsylvania, Clarion, PA 16214, USA

ARTICLE INFO

Keywords:
Facet
Orientation
SEM
Electron backscatter diffraction

ABSTRACT

Facets are flat faces of a single crystal, which are typically parallel to the low-energy lattice planes. The orienta-tion of a facet can sometimes be determined by simple visual examination, as in the case of the gemstone indus-try. Facets on microscale particles often do not correspond to the expected results of equilibrium, and the smaller physical size presents a challenge in observation. Using a facet observed on spherical particles of 20 μm diameter in alloys of $Al_{60}Cu_{25}Fe_{15}$ composition as an example, a procedure to determine facet orientation based on the combined usage of Scanning Electron Microscope (SEM) and Electron Backscatter Diffraction (EBSD) has been proposed and tested. Out of three types of facets found, the crystalline orientation of one type is determined by two approaches: by examination of facet relative layout and by orientation analysis based on the usage of SEM-EBSD. The former is along the traditional line of visual examination and the latter represents an attempt to ex-pand the application of EBSD in a different field. Both approaches proved that the surface of the facet is parallel to the {100} lattice plane of a cubic phase. The experimental details and the strength of SEM-EBSD in such appli-cation are discussed.

1. Introduction

It is well known that single crystals often have unique shapes defined by the relative layout of facets, which are faces smooth down to atomic level [1]. The arrangement of facets is closely related to the point symmetry of the crystal structure. It is generally accepted that the main driving force for the formation of facets is the reduction of surface energy. Studying facets gives us some insight about crystal structure and atomic bonding. On the other hand, facets affect the properties of materials. This is especially true for nano- and micro- particles, where the smaller size means increased ratios of surface to volume. Depending on which lattice plane a facet is terminated, properties, such as the activity of catalysts [2], will be different. Therefore, determination of facet crystalline orientation is important to both fundamental crystal structure study and to the application of micro- and nano- particles [3,4].

The crystalline orientation of facets can be determined by (a) simply observing the layout of facets and (b) relating the orientation of a facet relative to the crystal structure. The first approach takes advantage of the aforementioned relationship between crystalline point symmetry and the relative layout of facets [5]. Examination of the facet layout can be done by simple visual inspection when the crystal and facets are in macroscale. When they are in micro- to nano- meter order, usage of microscopes is necessary. Examples for microscopes are Atomic Force Microscope (AFM) [6], Scanning Electron Microscope (SEM) [7], and Transmission Electron Microscope (TEM) [8]. It should be pointed out that, in this approach, the value of experimental examination is more to confirm a suggested model. In contrast, the second approach is self-sufficient and can have some well-established steps to follow. The instruments for this purpose have to provide both morphology and crystal structure information. TEM satisfies this requirement. TEM is an excellent tool to study nanoparticles when specimen preparation can be accomplished by simple dispersion. The challenge of using TEM for this purpose is the specimen preparation when the particle is in micrometer order, which will be discussed later in conjunction with results of the current study. SEM is also a tool suitable for this purpose. The stage of a typical modern SEM is equipped with tilting and rotation functions, enabling the view of particles from different angles. With the addition of Electron Backscatter Diffraction (EBSD), direct crystal structure information can be obtained. The combination of the morphology and crystal structure information makes SEM-EBSD a promising tool in facet crystalline orientation analysis for particles of micrometer size, though it has not been fully explored.

* Corresponding author.
E-mail address: cli@clarion.edu (C. Li).

https://doi.org/10.1016/j.matchar.2022.112158
Received 28 April 2022; Received in revised form 15 July 2022; Accepted 22 July 2022
1044-5803/

The facet that will be studied in the present work is on spherical particles found in as-prepared alloy of $Al_{65}Cu_{25}Fe_{15}$ composition by arc melting. There have been extensive studies about this alloy, mainly because of the reports of successful preparation of a stable and single Icosahedral Quasicrystalline (IQC) phase [9,10]. However, follow-up studies have revealed that the constituent phases and microstructure of this alloy depend on the preparation and subsequent thermal processes very sensitively [11,12]. In an as-prepared alloy by arc melting, Balzuweit et al. [13] reported the presence of a β crystalline phase in spherical shape, instead of pure IQC phase. This report is confirmed by Cheung et al. [14]. In a more recent study, this spherical particle has been found to have more complicated structure and phases [15]. It has IQC particles as a core and is covered with a single crystal of β phase on the surface. Since the characterization techniques used in this study probes the surface layer only, we still consider the spherical particle as single crystal of β phase. β phase is of TiNi type cubic crystal system. Facets on the surface of the spherical particles have been reported, the formation of which depends on the thermal process sensitively. Therefore, the details of the facet, in return, could serve as a foot-print for the thermal process an alloy went through, which is very important for the study of this alloy. Despite its importance and the wealth of information it could bring in, there have been no dedicated studies regarding these facets.

In the present paper, using the facets mentioned above as an example, two approaches of studying facet orientation have been proposed and tested based on the combined usage of SEM and EBSD. The first approach is based on simple layout observation, while the second one relates EBSD data to morphology information of SEM images. The two approaches reached the same conclusion. It is further suggested that the second approach eliminates the speculation in the first one and can be used in a wide range of cases.

2. Experimental

The alloy was prepared by arc melting pure Aluminum (99.99%), Copper (99.9%), and Iron (99.9%) from Goodfellow with a nominal composition of $Al_{65}Cu_{20}Fe_{15}$. The chamber was evacuated to a vacuum of 10^{-5} Torr, purged and refilled with pure Ar gas. The alloy was cast into a water-cooled copper crucible. The button shaped alloy ingot has a diameter of 2 cm for its circular cross-section and a height of 1 cm. The as-prepared alloy is porous, consisting of multiple voids. The alloy was crushed to pieces of several ten micrometers in size to expose the surface of the voids, on which the spherical particles of interest were found.

Particle morphology examination was carried out by using a TESCAN Vega-3 XMU SEM with LaB_6 type emitter. The equipped Oxford Aztec symmetry EBSD system was used for facet crystalline orientation analysis. For both SEM imaging and EBSD analysis, the SEM was operated at an accelerating voltage of 10 kV. The electron beam diameter is controlled by choosing beam intensity. A smaller beam intensity number corresponds to a smaller electron beam diameter and weaker electron beam current. Beam intensity of five was used for SEM imaging and 15 was used for EBSD analysis. The SEM stage can be rotated 360°. A single tilting axis enables tilting of the specimen, the limit of which depends on the stage position with a typical value of 30° for regular SEM imaging. The combination of the two allows the observation of an object from a range of angles. However, as will be explained later, this range is not sufficient for the present work. A special specimen holder is assembled to extend the angle range.

3. Result and discussion

A typical SEM image of the spherical particle of interest is shown in Fig. 1(a). On the SEM image, the facets appear as different patterns, based on which they can be classified to three types and have been marked with markers of elliptical, triangular, and square shapes. Based on the consideration of cubic crystal structure for the sphere and the layout of different facets to be explained later, we propose the following model regarding the facets in relation with the crystalline orientation of the β phase. The facet marked with a square appears to be multiple concentric rings on the SEM image, which is actually a terrace-like structure in three dimensions. Each ring can be considered as the result of intersection between a plane parallel to the {1 0 0} lattice plane and the sphere. If we consider the particle is of perfect spherical shape, a line connecting the centers of the sphere and the center of the circular rings is parallel to the ⍰100⍰ crystalline direction. Along the <1 0 0> crystalline direction, there is four-fold rotational symmetry in the cubic crystal structure. Because of this, when viewed in a direction normal to this type of facets, the arrangement of other facets is expected to show four-fold rotational symmetry. Out of such consideration, this type of facet is marked with a square-shaped marker. Similar consideration about the nature of the facets and the choice of markers are adopted for other types of facets. Facets marked with elliptical-shaped markers correspond to two-fold rotational symmetry and those with triangular markers correspond to three-fold rotational symmetry. The present work focuses on the type of facet marked with a square, which corresponds to four-fold rotational symmetry.

In the first approach, the orientation of the spherical particle is adjusted so that the SEM image corresponding to the edge-on orientation of the central four-fold rotational symmetry facet can be taken and the expected symmetric layout can be examined. Here, edge-on orientation is defined as the case when the electron beam is normal to the planes of the facets. The procedure of orientation adjustment is explained as follows in conjunction with Fig. 2, which shows the same SEM image as that of Fig. 1(a) with different schematic drawings. In Fig. 2(a), the projected circle of the spherical particle is traced with dotted line. The facets around the central vertical line are of three-, four-, and three- fold rotational symmetries. Their surface normal can be considered as, for example, parallel to [111], [001], and $\left[\bar{1}\,\bar{1}\,1\right]$ directions, respectively. As a result, the centers of the three facets lie on a big circle of the sphere. The big circle is projected as an ellipse because the circle plane is not parallel to the electron beam. Vector OA starts from the center of the sphere, ends at the center of the four-fold rotational symmetry facet, and is the surface normal of the facet. On the SEM image, O is projected as the center of the traced circle. If OA is parallel to the electron beam, O and A overlap with each other. The fact that OA has finite length on the SEM image implies that the facet is not edge-on. The required stage rotation and tilt angles to bring the facet to be edge-on can be estimated by analyzing the SEM image as shown in Fig. 2(b). For the convenience of explanation, a coordinate system has been designed with the origin sitting at the center of the sphere. The x-, y-, and z- axes point toward right, up, and out of the paper, respectively. The x-axis is in the same direction as the SEM stage tilting axis, while the z-axis is in the same direction as the stage rotation axis. This coordinate system is considered to be fixed while the orientation of the spherical particle can be adjusted relative to this coordinate system. The inlet is a drawing of the big circle of the sphere involving the highest point O″ of the sphere and the facet center A. On the SEM image, O″, O′, and O overlap with each other. To obtain an edge-on view of the facet is equivalent to make OA coincide with the z-axis. This can be accomplished by the combined usage of stage rotation and tilting functions. The first step involves rotating the sphere by angle φ shown in Fig. 2(b) so that vector OA lies in the y-z plane. Then, OA can be brought to be parallel to the z-axis by tilting. Angle φ can be measured directly on Fig. 2(b). The necessary tilting angle θ can be calculated as shown in the inlet of Fig. 2(b). Consider the right triangle AO'O, $\vartheta = Sin^{-1}(O'A/OA)$. Here, O'A is the distance of O″A on the SEM image and can be measured directly. OA is the radius of the sphere, which is the same as the radius of the traced circle. For the specific case shown in Fig. 2, this procedure predicted that the SEM stage needs to be rotated clockwise by 47° and tilted by 19 ° to bring the

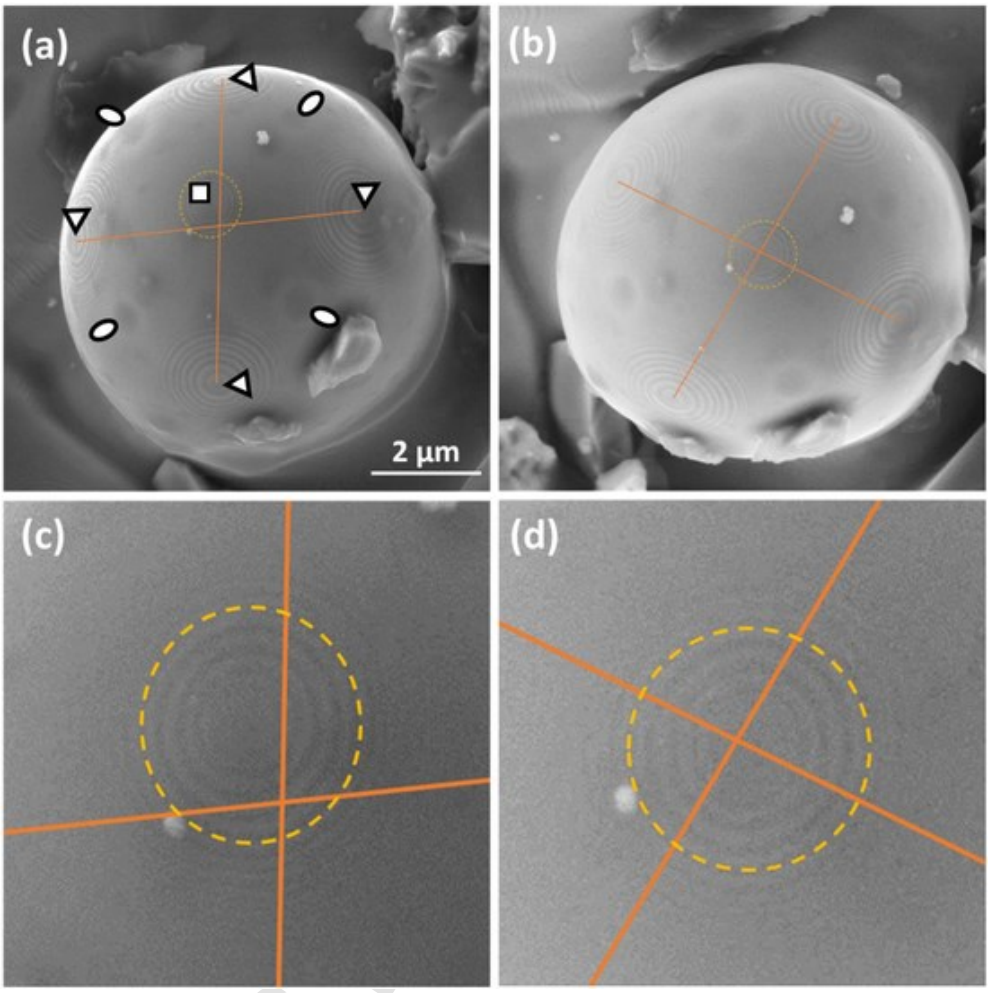

Fig. 1. SEM images of a typical spherical particle. (a) and (c) are SEM images before orientation adjustment while (b) and (d) are the images after adjustment. (c) and (d) are enlarged parts of (a) and (b), respectively.

central facet to be edge-on. A more detailed experimental examination found that a combination of 35 ° rotation and 17 ° tilt results in the best result. The criterion used to judge the accuracy of facet edge-on in fine-tuning is to maximize the area of the circles which is explained later. While the predicted and actual angles are very close for the tilting, the two values for the rotation are significantly different. Repeated trials found that the uncertainty comes from tracing the perimeter of the sphere with a circle on the SEM image. Our model assumes the particle is a perfect sphere while in reality, it is not; this leaves room for subjective judgement in the tracing operation. This uncertainty affects the direction of O″A and angle φ significantly. Its effect on the length of O″A and the radius of the circle is less significant. This is why the predicted rotation angle is less accurate as compared to the tilting angle. In summary, the suggested approach for orientation adjustment provided a rough road map for the rotation and tilting operation in the present case. The accuracy of this approach is limited and the best result is obtained by fine tuning the orientation to maximize the areas of the circles.

Fig. 1 shows the SEM images of the spherical particle before (a) and after (b) orientation adjustment. (c) and (d) are the corresponding enlarged images of the central parts, respectively. Based on our model, there are three criteria that can be used to judge if the four-fold rotational symmetry facet is edge-on. First, the centers of some facets, such as the two marked with triangles and the one with a square near the vertical line in Fig. 2(a), are on a big circle of the sphere. When the central facet is adjusted to be edge-on, the electron beam is parallel to the plane of the big circle. Then, the projection of the big circle is a straight line, on which the centers of the three facets are located. Similar consideration applies to the centers of facets near the horizontal line in Fig. 1 (a). Combining all these considerations, it is expected that the horizontal and vertical lines should intersect at the center of the four-fold rotational symmetry facet, when the central facet is edge-on. Judging based on this criterion, the facet in (b) and (d) is closer to being edge-on than that in (a) and (c). The second criterion is related to the circular shape of the concentric ring patterns. If we consider the rings to be perfectly circular in the edge-on orientation, they will be elliptical in any other orientation. Eccentricity for the circles on Fig. 1(c) is 0.36 while that for Fig. 1(d) is 0.29, indicating that the circles on Fig. 1(d) are closer to being perfect. The third criterion is related to the size. When the facet is edge-on, the area of a circle is expected to be the largest. Measurements obtained results consistent with this speculation. For example, ten measurements gave an average area of the circle traced with dotted line on Fig. 1(c) of 1.95 um^2 with a standard deviation of 0.02 um^2. Ten measurements of the same circle on Fig. 1(d) gave an average area of 2.08 um^2 with a standard deviation of 0.02 um^2. Measurement of other circles obtained very similar results in terms of both area size and eccentricity. The effectiveness of these three criteria have different dependency on the model. The first criterion is as good as the sphere approximation holds true. The second one depends on both the approximations of spherical shape for the particle and circular pattern for the facet. The third criterion does not depend on these and is believed to be universal, although it is not easy to figure out in what direction and how many degrees the rotation and tilting should be carried out. Nevertheless, in the present case, the judgements based on all three criteria are consistent in

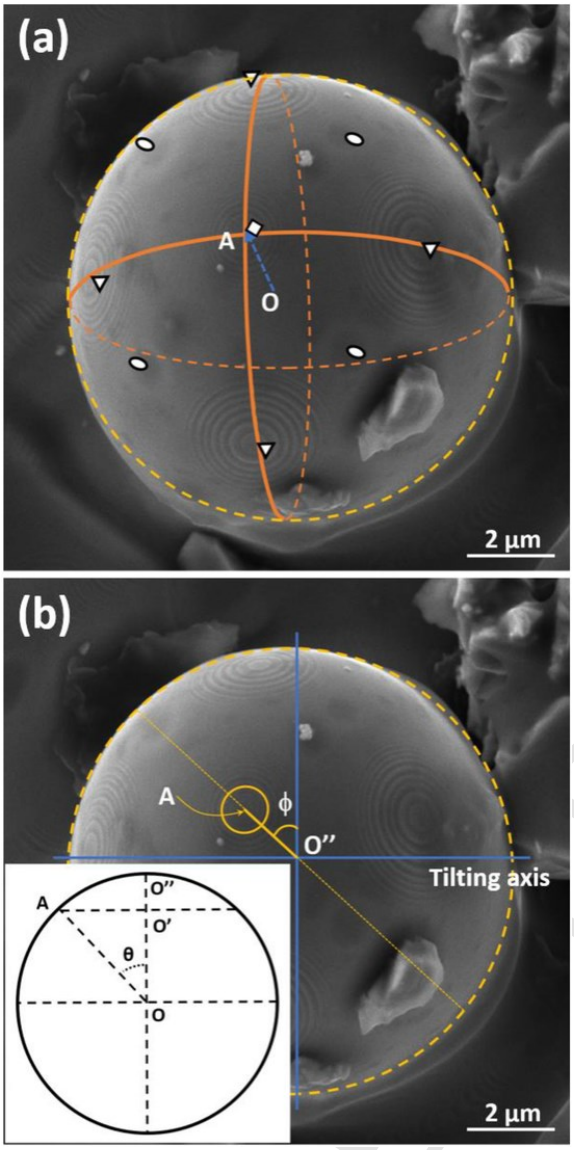

Fig. 2. SEM image of a spherical particle with four-fold rotational symmetry facet around the center. The schematic drawing in (a) shows that the centers of some facets are on big circles of the sphere. The schematic drawing in (b) shows how the rotation and tilt angles, which are required to make the central facet edge-on, are determined. The inlet in (b) is a drawing explaining the quantities needed to calculate tilting angle θ.

that the four-fold symmetry facet orientation in Figs. 1(b) and (d) is closer to being edge-on. As shown in Fig. 1(b), the arrangement of facets shows four-fold rotational symmetry, validating our hypothesis that the central facet is parallel to the {1 0 0} plane or normal to the $<1\ 0\ 0>$ crystalline direction.

This conclusion is verified by the second approach based on the usage of EBSD. For the analysis by EBSD, the specimen is tilted by 70° from the edge-on setting shown in Fig. 1(b), which is the typical practice for EBSD analysis [16]. The details of this experimental operation are explained later. Fig. 3 shows an SEM image of the spherical particle after tilting. Nearly all of the features can be traced back to that of Fig. 2 (b), ensuring that it is the same particle that is under analysis. The facet of interest is close to the very tip of the sphere. As shown by the enlarged inlet, the facet pattern is highly elongated in the horizontal direction, which is the direction of stage tilting axis. The elongation is expected because of the 70° tilting. Fig. 4(a) shows the EBSD patterns when electron beam is placed around the center of the facet. Fig. 4(b)

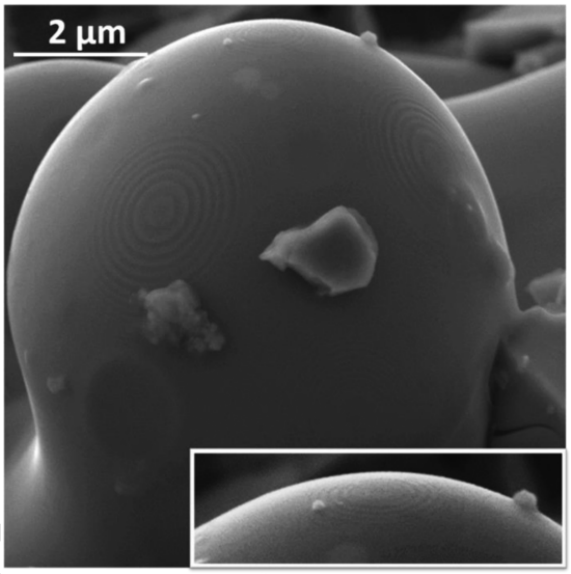

Fig. 3. SEM image of the spherical particle shown in Fig. 1(b) after tilting for 70° toward the EBSD detector. The four-fold rotational symmetry facet is on the tip and an enlarged image is shown in the inlet.

shows the same pattern with detected bands marked and Fig. 4(c) is one with the simulated pattern overlapped. The simulated pattern is generated by considering β phase of cubic structure with lattice constant reported in reference [17]. The agreement of the simulated and the detected patterns confirms the β phase crystal structure of the sphere. Further, a three-dimensional view of the cubic unit cell relative to the specimen surface, which is the flat surface of the four-fold rotational symmetry facet in this present case, is constructed and is shown in Fig. 4(d). Qualitatively, it can be seen that the specimen surface is parallel to the {1 0 0} lattice plane. Quantitatively, the orientation angles are (22.5°, 2.1°, 87.4°), from which the angle between the facet surface normal and that of the $<1\ 0\ 0>$ β phase crystalline direction is 2.1° [18]. It is considered that the 2.1° angle difference is due to experimental uncertainty. Therefore, it is concluded that the facet surface is parallel to the {1 0 0} lattice plane, again supporting our proposed model. Fig. 5 shows EBSD patterns taken from four different locations on the sphere. The patterns are displayed on top of the sphere according to the locations where they were taken. The pattern taken from the tip of the sphere has the best quality and is used for quantitative analysis in Fig. 4. EBSD patterns taken from other locations have portion or the whole area with reduced contrast due to the spherical geometric effect. Despite the quality difference, a close examination revealed that all the patterns have the same bands, implying that the sphere is of single crystal, confirming the previous report [15].

This paper presents two approaches to analyze the crystalline orientation of a facet: observation of facet layout and EBSD analysis. It is worthy to make a comparison of the two. In the present case, the hypothesis of facet symmetric arrangement depends on the assumption that the particle is of spherical shape. There are parts where the shape of the particle deviates from sphere. When this happens, the layout of the facets departs from the expected symmetry. Two examples are shown in Fig. 6. In Fig. 6(a), facets are marked with markers based on the same rule used in Fig. 1(a). We consider the facet layout centered on the one located in the right-upper corner and marked with triangle. Although this facet is not edge-on, the layout of the three adjacent facets marked with ellipses appears to have three-fold rotational symmetry. This symmetric arrangement is due to the spherical shape of the particle around this area. Moving further away from the chosen facet, facets marked with triangles are observed in the upper-left and lower-right corners. The layout of these two together with one not visible on this

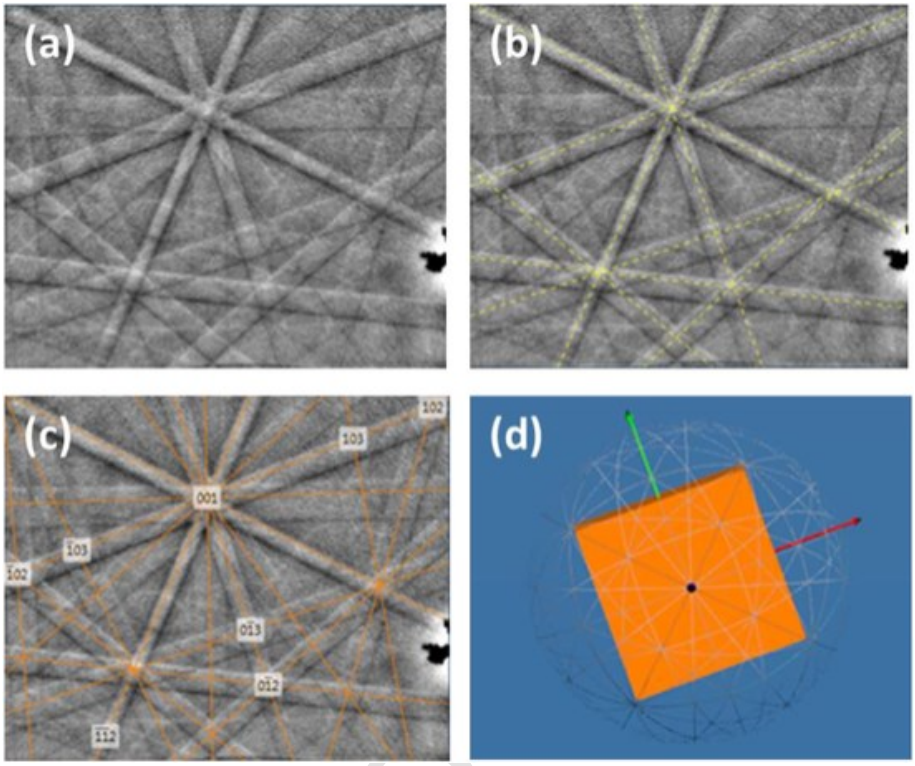

Fig. 4. EBSD pattern from the tip of the spherical particle in Fig. 3 and the results of analysis. (a) is the raw pattern, (b) is the pattern with detected bands marked, (c) is the pattern with simulated result overlapped, and the (d) is a three-dimensional view showing the crystalline orientation relative to the specimen coordinate.

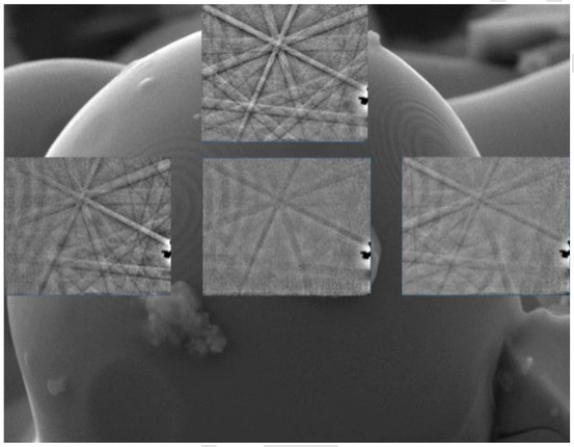

Fig. 5. EBSD patterns taken from different parts of the sphere. The locations of the patterns correspond to the points where electron beam is positioned to take the patterns.

image is expected to show three-fold rotational symmetry. However, the two do not resemble each other and do not appear to overlap with each other under three-fold rotational symmetry operation. This is because the surface morphologies of the particle at the locations of the two facets do not follow the spherical shape defined by that on the right-upper corner. Further, as shown with the trace-drawings, the rings of the facet on the right-lower corner do not have a shared center, which is a result of deviation of surface morphology from sphere locally. A more dramatic example is shown in Fig. 6(b). Here, one facet appears to have two centers. One possible explanation is that the particle is the result of two spherical particles fused together. Therefore, the first approach of facet orientation determination has limitation. On the other hand, the procedure of maximizing the area of a facet is universal. Once the plane(s) of facets are brought to be edge-on, it establishes a reference orientation. The facet can then be tilted in a controlled way to facilitate EBSD analysis, and the obtained EBSD pattern enables the determination of the crystalline plane parallel to the facet surface. Therefore, the second approach is universal. There are many factors that affect the uncertainty of the second SEM + EBSD approach. It is believed that the accuracy of setting-up the reference orientation plays important role. As discussed above, the ultimate criteria for judging a facet edge-on is the maximization of the area of a ring of the facet. The example of ring area measurement of 2.08 um^2 with a standard deviation of 0.02 um^2 shown in Fig. 1(d) can be used to estimate the uncertainty in this process. If we consider the area of the ring has a maximum of 2.08 um^2 when it is viewed along the surface normal, the area is decreased to 2.08 cos ($\Delta\vartheta$) μm^2 when it is viewed in a direction $\Delta\vartheta$ off from its surface normal. Based on this formula, when the area changes by one standard deviation, from 2.08 um^2 to 2.06 um^2, the corresponding $\Delta\vartheta$ value is 8°, which can be considered as the standard deviation of setting-up the reference orientation. Uncertainties also come from other factors: the errors associated with switching from the reference orientation to that suitable for EBSD analysis and the accuracy of EBSD analysis. It seems reasonable to consider the overall uncertainty of this method is in the order of 10°, which may not be ideal for facet analysis on some crystals. As discussed above, the precision of the ring area measurement plays important role, which can be improved by using field-emission SEM to obtain sharper SEM image and developing a computer program to measure the ring area automatically with higher accuracy.

This work demonstrated that the combination of SEM and EBSD is a unique and effective approach in analyzing facet crystalline orientation. A comparison of SEM-EBSD with TEM will make the point clear. If the facet in the present work is to be analyzed by using TEM, a specimen in the form of thin film must be prepared. This thin film must be extracted in a way such that it contains a significant portion of the surface of the facet and it must be perpendicular to the surface of the facet. The only possible way to prepare such a specimen is to use expensive modern dual-beam Focused Ion Beam (FIB) technology. Even with FIB, this task presents a very serious challenge. To protect the facet surface,

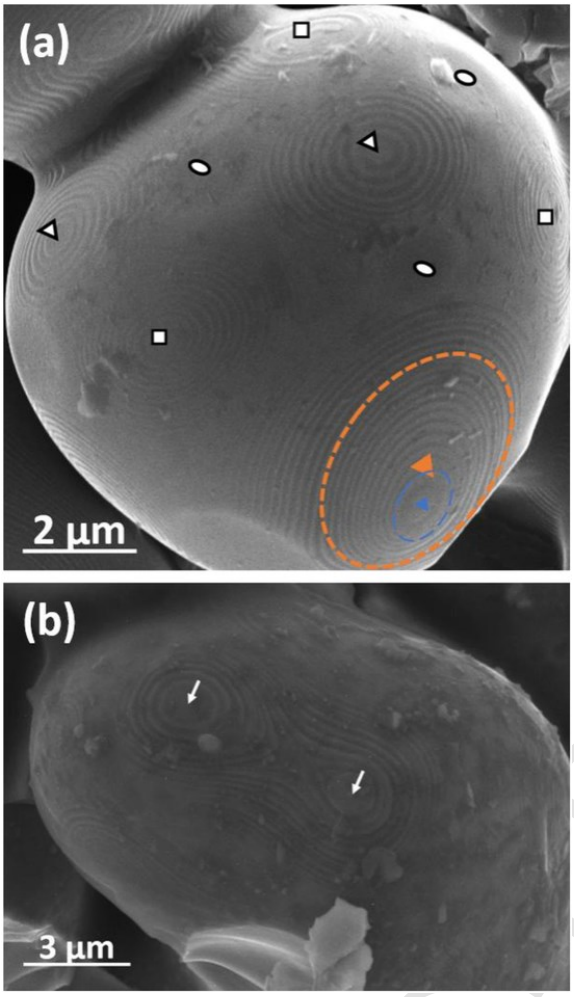

Fig. 6. SEM images showing the layout of facets on non-spherical particles. The drawings on the lower-right corner of (a) show that different rings of one facet have different centers and it is impossible to define a single center for the facet. The two arrows on (b) show the two centers for one facet.

the specimen must be coated, which makes locating the exact area difficult. Further, to make the edge-on SEM observation and to establish a reference orientation, the stage must be rotated and tilted. This will make switching from the SEM mode to FIB mode extremely difficult or nearly impossible. These multiple requirements reduce the rate of successful specimen preparation significantly. As a comparison, SEM-EBSD analysis, as we have demonstrated here, is all on the same instrument and is relatively easy to operate. Also, it is worthy to note that SEM-EBSD is inexpensive as compared to TEM and FIB. The present work expanded the usage of EBSD. It is a common belief that EBSD requires a flat smooth surface to obtain quality data. However, the specimen in the present study is of spherical shape. Instead of specimen preparation, this study made an effort in searching the suitable specimens. With these precautions taken, quality EBSD data has been obtained.

There are some experimental details that deserve more explanation. First, attention should be taken to choose particles that have higher elevation compared to the local terrain, to ensure the visibility of the object of interest after rotation and tilting. This is especially true for EBSD analysis since it involves large tilting angles. Second, since we have approximated the particle to be spherical, efforts should be made to choose those that resemble a sphere. A particle closer to being a perfect sphere will make the calculated rotation and tilting angles, as shown in Fig.2, more accurate. It also will enable an edge-on SEM image, such as those shown in Fig. 1(b), to present better expected symmetry of facet layout. Third, we spent time choosing the suitable facet, which is the four-fold symmetry one in the present case. The facet of interest should be close to the center of the projected circle of the sphere on the SEM image to start with, which implies that the necessary tilting angle is relatively small to bring the facet to edge-on orientation.

There are details in switching the facet orientation from edge-on for SEM observation to an orientation suitable for EBSD analysis. For the edge-on SEM observation, the specimen typically needs to be tilted by a smaller angle, 17 ° in the present case. From this edge-on orientation, the facet needs to be tilted typically 70 ° to facilitate EBSD analysis. The tilting requirement for EBSD is large, exceeding the tilting capability of most SEM. The following procedure is taken to address this problem. A SEM specimen holder with its own tilting function is assembled as shown in Fig. 7(a). The holder has more than 90° tilting capability, although it has to be done outside the SEM chamber. On top of the holder, a regular SEM stub is mounted. The stub can be rotated relative to the holder outside the SEM chamber. A piece of silicon wafer of rectangular shape and centimeter size is glued on top of the SEM stub. Double sided conductive tape is glued on top of the wafer, onto which the crushed particles are dispersed. The silicon wafer edge is straight and its orientation can be recorded with low-magnification SEM image as shown in Fig. 7(b). Such SEM image is comparable to image of optical microscope and the edge is used as a reference for consistent specimen orientation adjustment for the two orientations. Such an assembly is loaded into the SEM chamber with the holder tilting angle set at zero degree. Once a candidate of suitable facet is found, its orientation is adjusted by using SEM stage rotation and tilting functions so that the facet is edge-on and the rotation and tilting angles are recorded. The effect of stage rotation is recorded and reproduced by using the holder rotation function as follows. With the stage tilting set at zero degrees and rotation kept at the angle required for facet edge-on, a low magnification SEM image, comparable to optical microscope images in terms of magnification, is taken. This image is centered on the silicon wafer edge, an example of which is shown in Fig. 7(b). From this image, the angle between the straight edge and stage tilting axis can be measured. Then, the whole assembly is removed from SEM. Under an optical microscope with a video camera, the SEM stub on top of the assembled holder is readjusted so that the silicon wafer edge forms the same angle with the holder tilting axis. The direction of the holder tilting axis is represented by the edge marked as T in Fig. 7(a). In the subsequent reloading of the assembly, we made the holder tilting axis parallel to the stage tilting axis. This is done by adjusting the stage rotation so that the edge parallel to the holder tilting axis in Fig. 7(a) runs in horizontal direction on the SEM image. As a result of this operation, holder and stage tilting have the same effect. With the previously recorded stage tilt and rotation angles, we know at what holder tilting angle the facet of interest is edge-on. Another 70° tilt makes the facet surface suitable for EBSD analysis.

There are many unanswered questions regarding facets found in the present study. For example, as shown in Fig. 1, different types of facets have different appearances. While the facets corresponding to two-fold rotational symmetry appear to be a plain flat face, those corresponding to three- and four- fold rotational symmetries resemble multiple concentric rings. Further, the latter two differ from each other in terms of sizes and quantities of rings. It is valuable to find out how they quantitatively differ from each other and the reasons behind. Further, a close examination of some selected facets of three- and four- fold rotational symmetries revealed strong hints that they are polygon-shaped, not circular, as we have reasonably approximated. An example is shown in Fig. 8, where the assumed straight side of the central two rings have been drawn with dotted line on the inlet. Usage of a field emission SEM could give a more conclusive answer regarding the shapes and the gradual evolution from central polygon-resembling rings to outer circle-resemble rings. Application of SEM and EBSD, developed in the present work, will enable the determination of crystalline direction of the polygon sides.

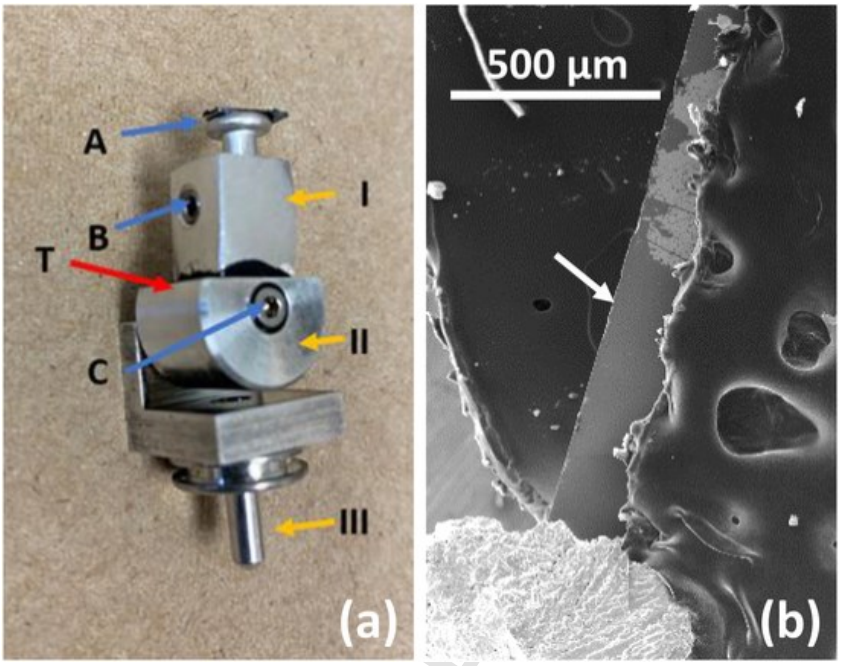

Fig. 7. A picture of the assembled special specimen holder (a) and a sample low magnification SEM image (b) of the silicon wafer edge for reference purpose. In (a), I, II, and III mark the three parts used to assemble the holder. Arrows of A, B, and C point to the silicon wafer, the set-screw for SEM stub, and the tilting axis screw, respectively. T marks the edge parallel to the holder tilting axis. In (b), the arrow points to the silicon wafer edge, which is used as a reference in switching orientations from edge-on SEM observation to that for EBSD analysis.

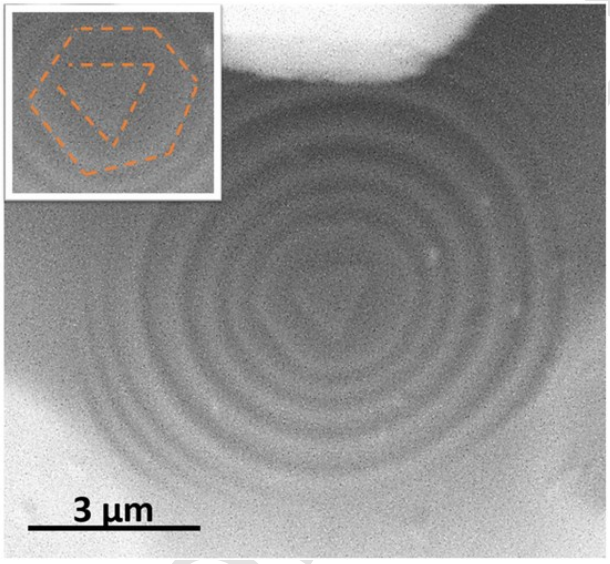

Fig. 8. A SEM image of facet with the central rings resemble polygon. The inlet shows the central part with straight sides traced.

4. Conclusion

Facets found in spherical particles of as-prepared alloy of $Al_{60}Cu_{25}Fe_{15}$ composition by arc melting are classified to three types based on their appearance. The crystalline orientation of one type of facets, corresponding to four-fold rotational symmetry, has been studied by two approaches. Examination of the facet layout on the SEM image taken when the facet is edge-on, enables us to conclude that the surface of this type of facet is parallel to the {1 0 0} lattice plane of the cubic β phase. In the second approach, the facet surface is analyzed by using EBSD, which provides direct evidence for the parallel relationship between the facet surface and the {1 0 0} lattice plane. Procedures have been proposed and tested to bring a facet to edge-on orientation, which is important for both approaches. The criterion of maximizing facet surface area in judging the degree of facet edge-on is suggested to be effective universally. A special specimen holder has been developed and a procedure has been proposed to tilt a facet surface by a large angle to facilitate EBSD analysis from the reference edge-on orientation. It is suggested that this combination of SEM imaging and EBSD analysis is very effective in analyzing a facet crystalline orientation.

Data availability

The raw/processed data required to reproduce these findings cannot be shared at this time due to technical or time limitations.

Declaration of Competing Interest

he authors declare that they have no known competing financial interests or personal relationships that could have appeared to influence the work reported in this paper.

Data availability

The authors are unable or have chosen not to specify which data has been used.

Acknowledgments

Financial support from National Science Foundation (DMR-1900077) is acknowledged.

References

[1] C. Hammond, The Basics of Crystallography and Diffraction, 2nd edn, 2002, pp. 1–5.
[2] J. Li, Z. Liu, D.A. Cullen, W. Hu, J. Huang, L. Yao, et al., Distribution and valence state of Ru species on CeO2 supports: support shape effect and its influence on CO oxidation, ACS Catal. 9 (12) (2019) 11088–11103.
[3] G.D. Barmparis, Z. Lodziana, N. Lopez, I.N. Remediakis, Nanoparticle shapes by using Wulff constructions and first-principles calculations, Beilstein Journal of

Nanotechnology 6 (1) (2015) 361–368.
[4] Y. Sun, Y. Xia, Shape-controlled synthesis of gold and silver nanoparticles, science 298 (5601) (2002) 2176–2179.
[5] C. Hammond, The Basics of Crystallography and Diffraction, vol. 21, International Union of Crystal, 2015, pp. 1–4.
[6] M. Schick, H. Dabringhaus, K. Wandelt, Macrosteps on CaF2 (111), J. Phys. Condens. Matter 16 (6) (2004) L33.
[7] J.J. M□tois, J.C. Heyraud, SEM studies of equilibrium forms: roughening transition and surface melting of indium and lead crystals, Ultramicroscopy 31 (1) (1989) 73–79.
[8] G. Liu, J. Li, K. Chen, Combustion synthesis of ceramic powders with controlled grain morphologies, Intech Open Access Publisher (2011) 49–74.
[9] A.P. Tsai, A. Inoue, T. Masumoto, Preparation of a new Al-Cu-Fe quasicrystal with large grain sizes by rapid solidification, J. Mater. Sci. Lett. 6 (12) (1987) 1403–1405.
[10] A.P. Tsai, Discovery of stable icosahedral quasicrystals: progress in understanding structure and properties, Chem. Soc. Rev. 42 (12) (2013) 5352–5365.
[11] C. Dong, J.M. Dubois, M. De Boissieu, C. Janot, Neutron diffraction study of the peritectic growth of the Al65Cu20Fe15 icosahedral quasi-crystal, J. Phys. Condens. Matter 2 (30) (1990) 6339.
[12] R. van Buuren, J. Sietsma, A. Van den Beukel, Crystallization of the "stable" quasicrystal AlCuFe, Mater. Sci. Eng. A 134 (1991) 951–954.
[13] K. Balzuweit, H. Meekes, G.V. Tendeloo, J.L. De Boer, On the relationship between morphology, composition and structure of Al-Cu-Fe crystals and quasicrystals, Philos. Mag. B 67 (4) (1993) 513–532.
[14] Y.L. Cheung, K.C. Chan, Y.H. Zhu, Characterization of the icosahedral phase in as-cast quasicrystalline Al65Cu20Fe15 alloy, Mater. Charact. 47 (3–4) (2001) 299–305.
[15] C. Li, C. Carey, D. Li, M. Caputo, R. Bouch, H. Hampikian, A study on spherical particles in Al65Cu20Fe15 alloy prepared by arc melting, Mater. Charact. 140 (2018) 162–171.
[16] S.I. Wright, in: A.J. Schwartz, M. Kumar, B.L. Adams, D.P. Field (Eds.), Electron Backscatter Diffraction in Materials Science, vol. 2, Springer, New York, 2009, pp. 51–61.
[17] F.W. Gayle, A.J. Shapiro, F.S. Biancaniello, W.J. Boettinger, The Al-Cu-Fe phase diagram: 0 to 25 At. pct Fe and 50, Metall. Trans. A. 23 (9) (1992) 2409–2417.
[18] K. Rajan, in: A.J. Schwartz, M. Kumar, B.L. Adams, D.P. Field (Eds.), Electron Backscatter Diffraction in Materials Science, vol. 2, Springer, New York, 2009, pp. 31–38.